JACS
JOURNAL OF THE AMERICAN CHEMICAL SOCIETY
Article
pubs.acs.org/JACS

Lanthanide-Chelating Carbohydrate Conjugates Are Useful Tools To Characterize Carbohydrate Conformation in Solution and Sensitive Sensors to Detect Carbohydrate−Protein Interactions

Ángeles Canales,[†] Álvaro Mallagaray,[‡] M. Álvaro Berbís,[‡] Armando Navarro-Vázquez,[∥] Gema Domínguez,[§] F. Javier Cañada,[‡] Sabine André,[#] Hans-Joachim Gabius,[#] Javier Pérez-Castells,[§] and Jesús Jiménez-Barbero*[,‡]

[†]Department of Química Orgánica I, Fac. C.C. Químicas, Universidad Complutense de Madrid, Avd. Complutense s/n 28040, Madrid, Spain

[‡]Department of De Biología Físico-Química, Centro de Investigaciones Biológicas, CSIC, 28040, Madrid, Spain

[#]Institute of Physiological Chemistry, Faculty of Veterinary Medicine, Ludwig-Maximilians University, 80539, Munich, Germany

[§]Faculty of De Farmacia, Department of Química, Universidad CEU San Pablo, Urb. Montepríncipe, ctra. Boadilla del Monte, 28668, Madrid, Spain

[∥]Department of Química Orgánica, Universidade de Vigo, Campus Universitario Vigo, 36310, Pontevedra, Spain

Supporting Information

ABSTRACT: The increasing interest in the functional versatility of glycan epitopes in cellular glycoconjugates calls for developing sensitive methods to define carbohydrate conformation in solution and to characterize protein−carbohydrate interactions. Measurements of pseudocontact shifts in the presence of a paramagnetic cation can provide such information. In this work, the energetically privileged conformation of a disaccharide (lactose as test case) was experimentally inferred by using a synthetic carbohydrate conjugate bearing a lanthanide binding tag. In addition, the binding of lactose to a biomedically relevant receptor (the human adhesion/growth-regulatory lectin galectin-3) and its consequences in structural terms were defined, using Dy^{3+}, Tb^{3+}, and Tm^{3+}. The described approach, complementing the previously tested protein tagging as a way to exploit paramagnetism, enables to detect binding, even weak interactions, and to characterize in detail topological aspects useful for physiological ligands and mimetics in drug design.

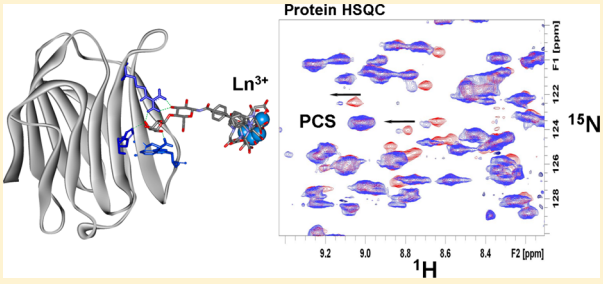

INTRODUCTION

Nature has endowed carbohydrates with exceptional properties for coding information, and indeed, a sophisticated enzymatic machinery has been developed for highly regulated biosynthesis of complex glycans.[1] This also holds true for receptors (lectins), which translate the sugar-based signals into cellular effects.[1,2] Addressing the challenge of structural characterization of protein−carbohydrate recognition in detail will not only give a functional meaning to distinct aspects of the glycome but will also be the basis to develop potent inhibitors, e.g., to block bacterial/viral infections or dysfunctional growth regulation in inflammation/tumor progression. This biomedical perspective explains the attention given to developing reliable and sensitive methods to explore carbohydrate structure, dynamics, and recognition.

Solution NMR spectroscopy is a major tool to characterize these properties. In fact, different NMR approaches are widely employed to study the interactions of carbohydrates and chemical analogues (glycomimetics)[3,4] with their receptors up to the level of atomic resolution, both from the perspective of the carbohydrate ligand[5] and from the receptor.[6,7] A widely popular strategy takes advantage of *J*-couplings or magnetization transfer processes, related to intra- or intermolecular nuclear Overhauser (NOE) enhancements,[8] although the use of other sources of information, for instance, residual dipolar couplings (RDCs), has also been described.[9,10] The growing insight into physiological glycan functionality via lectin binding is a strong incentive to broaden the scope of respective analytical procedures. When planning to develop new methods, the special features of carbohydrates as ligands deserve to be considered. Carbohydrates are flexible molecules that can adopt a variety of shapes in solution and bind in a certain geometry to their particular receptors.[11] Their binding strengths to proteins are usually rather weak, unless multivalent effects are involved.[12] In most cases, despite an exquisite selectivity of protein−carbohydrate interactions, dissociation constants are typically in the mM to low μM range.[13] Also of note, there are often

Received: March 13, 2014
Published: May 15, 2014

   dx.doi.org/10.1021/ja502406x | *J. Am. Chem. Soc.* 2014, 136, 8011−8017

problems in obtaining structural information on these systems by NOEs, due to signal overlapping, strong coupling, and/or the scarcity of key NOE information.[14] Moreover, few intermolecular carbohydrate−protein NOEs are usually detected, hampering the structure calculation of carbohydrate−protein complexes at high resolution.[11] Therefore, the NMR-based structural characterization at atomic resolution of protein−carbohydrate complexes is not a trivial task. As consequences, from the NMR perspective, there is an obvious need for introducing additional NMR parameters that can be reliably employed to monitor and study the conformation of complex carbohydrates and their interactions with receptors. Paramagnetic ions offer this potential. Historically, the presence of Mn^{2+} as an integral part in a plant lectin, which is essential for activity, served as starting point for measuring magnetic relaxation dispersion or line broadening.[15]

The use of paramagnetic ions exploiting lanthanide binding tags (LBT) to obtain new NMR parameters providing structural information has been extended in the past few years for protein structure determination.[16−18] The access to pseudocontact shifts (PCS), paramagnetic relaxation enhancements (PREs), and even to residual dipolar couplings (RDC)[19] has permitted to deduce key conformational and dynamic information in different elegant examples. In the study of protein−carbohydrate interactions, Prestegard and co-workers have made relevant contributions employing either spin-labeled sugar molecules[20] or measuring RDC parameters in chemically modified proteins, either with short alkyl chains,[21] histidine tags,[22] or lanthanide-binding peptides.[23] Using a human lectin, known for its role in infection, inflammation, pro-tumoral processes, and glycoprotein routing, i.e. galectin-3,[24−29] genetic engineering led to a construct of lectin and chelating peptide at the C-terminus.[23] This hybrid combined capacity for sugar binding with topological fixation of the lanthanide.

In a molecular recognition context, from the receptor's perspective, a paramagnetic protein tagging approach has been recently implemented for fragment-based ligand screening.[30]

In comparison, few examples have taken the alternative approach, i.e., tackling the problem from the ligand's perspective. We[31] and others[32,33] have recently reported on the use of a chemically well-defined lanthanide binding tag, to perform structural studies of carbohydrates in the free state, with the final aim of also performing molecular recognition studies. Our initial design[31] consisted of a 1-β-aminochitobiose moiety bearing a rigid linker attached to the 1-amino group, with a biphenylic EDTA lanthanide-chelating unit. The 7.1 Å length of the biphenyl moiety positions the metal ion more than 10 Å away from the sugar moiety in the conjugate, thus minimizing PRE in the NMR-active carbohydrate atoms. This long distance to the metal center causes the observed chemical shift changes that would be primarily due to the pseudocontact, rather than contact shift mechanism. Very satisfactory results were obtained, and the measurement and analysis of the PCSs validated the conformational behavior of *N*,*N*′-diacetyl chitobiose, the disaccharide repeating unit of chitin. This example also allowed to demonstrate that the attached LBT at the reducing end does not modify the shape of the disaccharide entity. However, from the chemical perspective, this compound presents a stereogenic center at the chelating unit, which complicates the synthetic process.

Herein, we present the synthesis of a second generation of carbohydrate derivatives with a novel lanthanide-binding tag and its application for conformational analysis of carbohydrates. Equally important, we also provide a proof-of-principle example that these derivatives can be efficiently used to monitor carbohydrate−protein interactions, providing structural information on the binding event at the protein receptor. Of note, depending on the choice of the metal ion at the tag, the magnitude of the paramagnetic effects can be modulated, facilitating access to a variety of structural data. To enable comparison between methods, we have deliberately tested human galectin-3, also offering a biomedically relevant study object. In addition, this approach does not require the preparation of protein mutants, thus allowing the study of the protein in its native form.

METHODS

PCSs Measurements. Experimental PCSs for the lanthanide-chelating carbohydrate derivative were calculated as the difference between the chemical shift of each signal in a $^{1}H-^{13}C$ HSQC spectrum acquired in the presence of a diamagnetic metal ion (La^{3+}) and a spectrum acquired in the presence of a paramagnetic metal ions (Tb^{3+}, Dy^{3+}). Spectra were acquired with 16 scans, 2000 and 256 complex points in ^{1}H and ^{13}C dimensions, respectively, at 11.7 T and 298 K. Samples were prepared in deuterated Tris buffer (D_2O, hexadeuterated Tris, 50 mM, pH 7.8) at a final concentration of the carbohydrate derivative **5** of 2.5 mM. CH_3CN (2 μL) was added as chemical shift reference.

Once the experimental values were obtained, a development version of Mspin software[34] was used to back-calculate the expected PCSs from the different lactose conformations. The existence of one major and two minor conformations around the glycosidic angles of lactose in solution has been previously described in detail.[35−39] An ensemble of lactose conformations was built taking into account both the described conformers around the glycosidic linkages and the flexible torsions of the linker.[32,35−39] Three conformational families were built for the lactose conjugate according to the Φ and Ψ dihedral angles values, namely syn Φ/syn Ψ, anti Φ/syn Ψ, and syn Φ/anti Ψ (see below) . The geometry of the phenylene diamino tetraacetic chelating unit was obtained from the reported X-ray coordinates for this moiety.[40] The quality of the fitting between experimental and back-calculated values is given by the Cornilescu's *Q* factor, which is defined by the following expression:[34]

$$Q = \sqrt{\frac{\sum (\mathrm{PCS}_{\mathrm{calc}} - \mathrm{PCS}_{\mathrm{exp}})^2}{\sum \mathrm{PCS}_{\mathrm{exp}}{}^2}}$$

For molecular recognition applications, the ability of our lanthanide-chelating lactose-derivative to be specifically recognized by Gal-3 was studied by saturation transfer difference (STD),[41] an NMR technique that is based on the transfer of magnetization from the irradiated protein to its binding ligands and provides epitope information at the ligand level. Samples for STD experiments contained 1 mM of the lanthanide chelating lactose-conjugate and 30 μM of human gal-3 CRD in deuterated Tris buffer, pH 7.8. NMR data were collected at 298 K on a Bruker Avance DRX 500 MHz spectrometer equipped with a 5 mm inverse probe head. The protein was saturated on-resonance at 0.5 ppm and off-resonance at 100 ppm with a train of Gaussian-shaped pulses of 50 ms each and a total saturation time of 2 s. A spin-lock field of 5 kHz with a duration of 15 ms was applied to minimize the protein signal background.

Galectin-3 PCSs were measured from $^{1}H-^{15}N$ HSQC experiments acquired in the presence of the lanthanide chelating carbohydrate conjugate loaded either with diamagnetic (La^{3+}) or with paramagnetic ions (Tm^{3+}, Dy^{3+}). The spectra were recorded with 48 scans, 1024 and 128 complex points in ^{1}H and ^{15}N dimensions, respectively, at 14.1 T and 298 K. Samples were prepared in deuterated Tris buffer (D_2O, hexadeuterated Tris, 50 mM, pH 7.8). The protein concentration was 270 μM, and the lactose derivative/protein molar ratio was set to 12/1.

For analyzing the lectin PCSs, MSpin software was also used to back-calculate the expected PCSs for the geometry reported in the

dx.doi.org/10.1021/ja502406x | J. Am. Chem. Soc. 2014, 136, 8011−8017

X-ray crystallographic structure of the galectin-3/lactose complex (PDB code 2NN8). The lactose molecule of the X-ray structure was replaced by the lactose conjugate bearing the lanthanide-binding tag, and an ensemble of lactose structures was built, as described above, to consider the flexibility of the linker.[42] The geometry of the phenylene diamino tetraacetic unit was taken from the reported coordinates of this moiety crystallized in the presence of Fe(III).[40]

RESULTS AND DISCUSSION

Synthesis of the Lanthanide Chelating Carbohydrate Conjugate. This second-generation lanthanide-carbohydrate conjugate is the straightforward extension of the phenylene diamino tetraacetic unit (PhDTA), which has been recently used as chelating unit for caged lanthanide complexes in NMR studies.[42] Although shorter than our initial design, this structure positions the metal at more than 10 Å from the carbohydrate moiety, further away than the monoaromatic precursor. This length permits to obtain PCS values from both sugar rings of the disaccharide, as will be described below.

The synthesis of the lactose derivative **5** was planned in a convergent way. 1-β-Aminolactose was obtained by synthesizing hepta-*O*-acetylated 1-β-aminolactose from 1-β-azide lactose followed by deacetylation, thus obtaining the desired disaccharide in a 75% yield.[32] The synthesis of the linker was based on a Suzuki coupling of an aryl boronate with protected *p*-iodobenzoic acid. We chose trimethylsilylethyl (TMSE) as protecting group for the carboxylic acid because it can be selectively cleaved in the presence of *tert*-butyl esters and is highly stable under Suzuki conditions.

First, we prepared the PhDTA fragment. Initially, we used 4-bromophenylenediamine as starting material, which upon extensive N-alkylation with *tert*-butylbromoacetate gave the trialkylated derivative **1** as the major reaction product. No reaction conditions afforded the desired tetraacetate derivative. Therefore, we decided to start with *o*-phenylenediamine and to prepare compound **2** followed by a bromination reaction.

This intermediate **2** was prepared (83% yield) under similar alkylation conditions, with traces of other alkylation subproducts, which could be separated. The use of acetonitrile as solvent was critical as the alkylation of phenylenediamine in toluene or DMF provided only low yields of mixtures of mono-, di-, and trialkylated products. Bromination of **2** (Scheme 1) with KBr/Oxone gave **3** as a single regioisomer (78% yield).

The next step was a tandem boronation-Suzuki coupling, which, after an extensive study of the reaction conditions (see Supporting Information), afforded the bicyclic product **4** in a 75% overall yield. The TMSE group was selectively deprotected in the presence of TBAF affording the corresponding acid in 86% yield, which was condensed with 1-β-aminolactose in the presence of HATU and DIPEA. The final carbohydrate derivative **5** was obtained upon hydrolysis of the *tert*-butylesters. All the condensations and hydrolysis steps proceeded with good yields (Scheme 2).

Assessing the Conformation of Lactose by PCSs. The first step in the analysis concerned the employment of PCSs to assess the conformation of the lactose-containing molecule in water solution and to demonstrate that the shape of the disaccharide is not affected by the presence of the LBT. Thus, PCSs of the lactose derivative **5** were obtained by comparing the ^{13}C and ^{1}H NMR chemical shifts of **5** in the presence of diamagnetic (La^{3+}) and paramagnetic (Tb^{3+}, Dy^{3+}) ions, through the use of standard $^{1}H-^{13}C$ HSQC experiments, as

Scheme 1. Synthesis of the PhDTA Chelating Unit Selectively Brominated

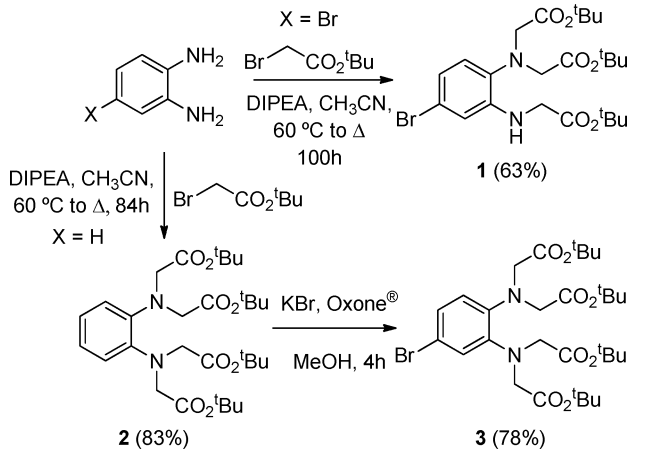

Scheme 2. Synthetic Scheme of the Boronation-Suzuki Coupling Leading to the Lactose Tag

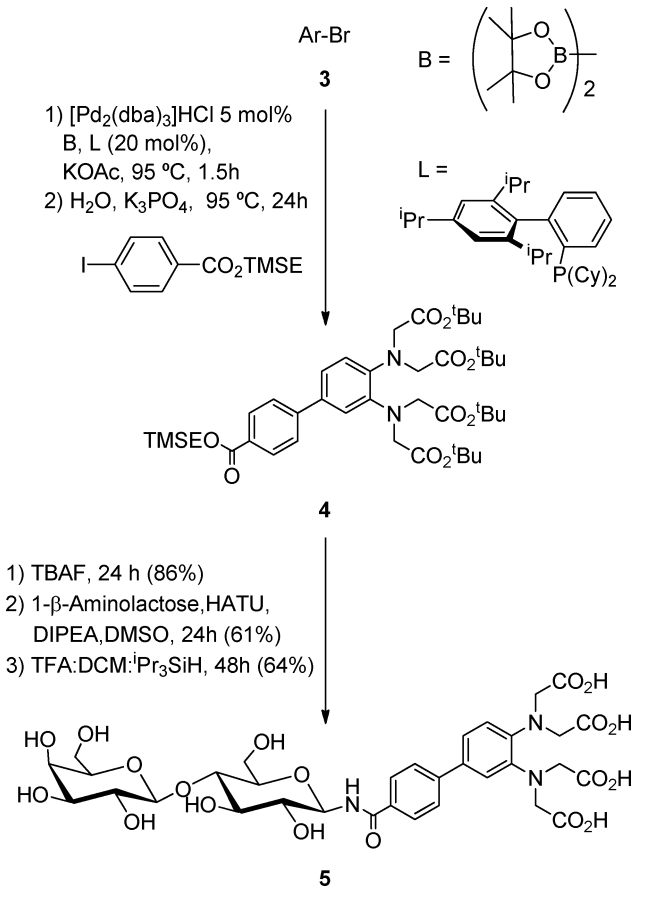

described in the Methods section. Fittingly, only one set of NMR signals was observed for the molecule in the presence of stoichiometric amounts of the metal. Inspection of the cross peaks permitted to demonstrate that all the carbohydrate NMR signals could be detected. Therefore, this linker is long enough to restrict PREs effects to the linker NMR signals.

Significant induced ^{1}H and ^{13}C PCS could be observed in the sugar even above 1 ppm for Glc H-1 (the sugar hydrogen closest to the metal, $\Delta PCS = +1.78$ ppm for Dy^{3+} and $\Delta PCS = +0.94$ ppm for Tb^{3+}, see Figure 1).

dx.doi.org/10.1021/ja502406x | J. Am. Chem. Soc. 2014, 136, 8011−8017

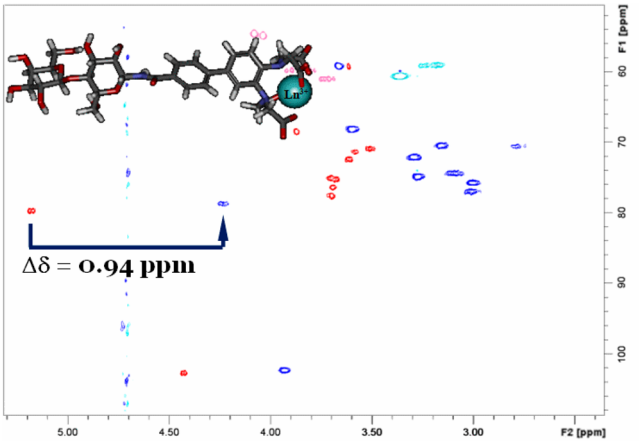

Figure 1. Superimposition of the $^{1}H-^{13}C$ HSQC spectra obtained for **5** acquired in the presence of a diamagnetic metal (La^{3+}, red) and in the presence of a paramagnetic metal (Tb^{3+}, blue). The PCS (0.94 ppm) or Glc H-1 is highlighted.

The experimental PCSs were then used to infer the solution conformation of the lactose moiety around the glycosidic torsion angles and to ascertain the presence of the typical chair conformation for the two pyranose rings also in the presence of the LBT. Different studies have concluded that the conformation of lactose can be described by two $^{4}C_{1}$ chairs for the Gal and Glc rings along with a major conformation around the glycosidic torsion angles, Φ (H1−C1−O−C4) and Ψ (C1−O−C4−H4).[35−39] This conformation (synΦ/synΨ), favored by the exoanomeric effect,[43] is described by Φ/Ψ torsion angle values of ∼55°/0°. Two other very minor conformations have been detected, with proportions smaller than 5%, with torsion angle values around 180° (anti) either for Φ or for Ψ, thus establishing antiΦ/synΨ or synΦ/antiΨ conformers, respectively.[35−39]

MSpin calculations[34] were performed to deduce the expected PCSs, using as input the coordinates of the three basic geometries of the lactose conformers mentioned above and the X-ray coordinates for the LBT[40] in the presence of Tb^{3+} and Dy^{3+}. Moreover, in order to take into account the linker flexibility, four different staggered conformations of the biphenyl moiety and two staggered positions of the amide bond with respect to the adjacent aromatic ring were built. Therefore, eight structures were calculated for each Φ/Ψ conformer. The backcalculated PCSs were fairly similar for all the rotamers since, as expected from the design, the rotation around these bonds did not substantially alter the metal position with respect to the sugar moieties. A representation of the flexibility of the linker is given in Figure 2a for the major synΦ/synΨ conformer.

Fittingly, the back-calculated PCSs obtained with the major conformer (synΦ/synΨ) were in excellent agreement with the experimental data (see Figure 2). The *Q* quality factor obtained from the MSpin calculations is 0.06 for Dy^{3+}, considering both the ^{1}H and ^{13}C NMR data.

SVD-based computations (see Supporting Information for details) were also performed using the MSpin software[34] to fit the observed ^{1}H and ^{13}C PCSs. As input coordinates, the three conformational families of the tagged lactose conformers mentioned above and the X-ray coordinates of the LBT[40] were employed. In the presence of Tb^{3+} and Dy^{3+}, the major conformer geometry (synΦ/synΨ) furnished *Q* quality factors

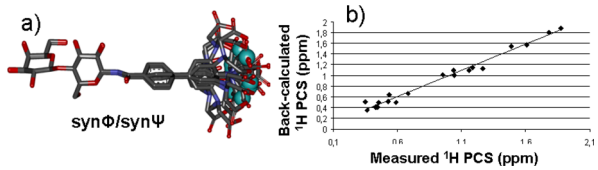

Figure 2. ^{1}H and ^{13}C PCSs correlation plots (b) for the fitting of the experimental data to the back calculated data for the geometry of **5** loaded with Dy^{3+}, built from the major lactose conformation (a). Eight structures were considered for each conformer (synΦ/synΨ, antiΦ/synΨ, or synΦ/antiΨ) in the calculations, two staggered conformations of the amide respect to the aromatic ring attached and four conformations around the bond connecting both aromatic rings of the biphenyl were used.

in a 0.064−0.068 range, see Figure 2. The value for the synΦ/antiΨ conformations was markedly deviated ($Q = 0.108-0.139$), while the antiΦ/synΨ conformers also provided a poorer fitting ($Q = 0.079-0.086$).

It is worth noting that since metal-proton vectors span a narrow angle, the SVD problem is not well-conditioned, with the corresponding condition numbers in the order of 100. This means that the $\Delta\chi$ tensor can not be fully determined from the available experimental data. However, since the metal-nuclei vectors span similar angles in the three conformations, discrimination between them is possible even when some elements of the $\Delta\chi$ tensor are not well-defined. A bootstrapping analysis of the Dy^{3+} data,[44] assuming a Gaussian error of 0.01 ppm in the experimental measurements, was then carried out in order to check if the *Q* factor difference obtained between the three conformational families showed statistical significance. It was observed that the ΔQ difference between quality factors was kept nearly constant ($\sigma \sim 0.001$) among the different samples. Hence, our PCS results agree with existence of one very predominant conformation around the synΦ/synΨ glycosidic linkages of lactose as stated before.[35−39] This conclusion, which has been deduced by using a variety of experimental and theoretical methods,[38,39] differs from that recently reported,[32] using a similar approach to that described herein. In that work, the authors indicated that it was necessary to include several lactose conformations to fit the experimental data.

Molecular Recognition: The Interaction of 5 with the Carbohydrate Recognition Domain of Human Galectin-3 (hGal-3). It is well-established that molecular recognition events in solution can be followed by using NMR, from either the ligand's or the receptor's perspectives.[45]

We first tested the ability of **5** to be specifically recognized by the human Gal-3 carbohydrate recognition domain (hGal3 CRD). As a first step, titration experiments were carried out both with natural lactose (as blank experiment) and with the lactose derivative **5** for comparison. The dissociation constants obtained with both ligands are equivalent (see Supporting Information).

In addition, we used STD-NMR.[41] STD experiments represent a straightforward means to explore, at atomic resolution, that the ligand epitopes responsible for the recognition process by hGal3 were the same.

The rise of STD signals in the corresponding experiment demonstrated the recognition of **5** by the lectin (Figure 4). In addition, inspection of the STD profile revealed a higher degree of magnetization for the hydrogen nuclei belonging to the lactose moiety (Figure 4B), leaving the linker and chelating region comparatively much less affected. The highest degree of

dx.doi.org/10.1021/ja502406x | J. Am. Chem. Soc. 2014, 136, 8011−8017

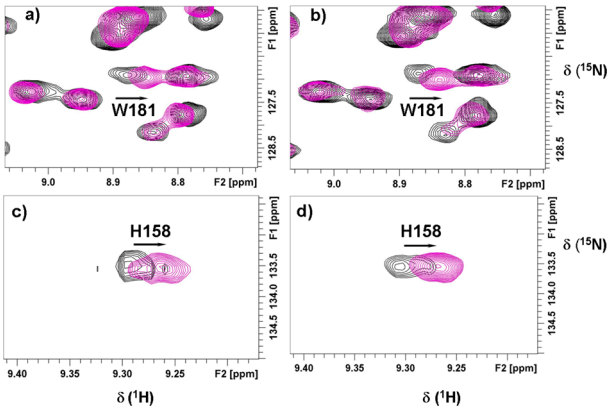

Figure 3. Right panels: $^{1}H-^{15}N$ HSQC (acquired at 700 MHz) for the galectin-3:lactose (molar ratio 1:12) sample. Left panels: $^{1}H-^{15}N$ HSQC (acquired at 600 MHz) for the sample containing galectin-3 and the lactose derivative **5**, loaded with La^{3+} (molar ratio 1:12).

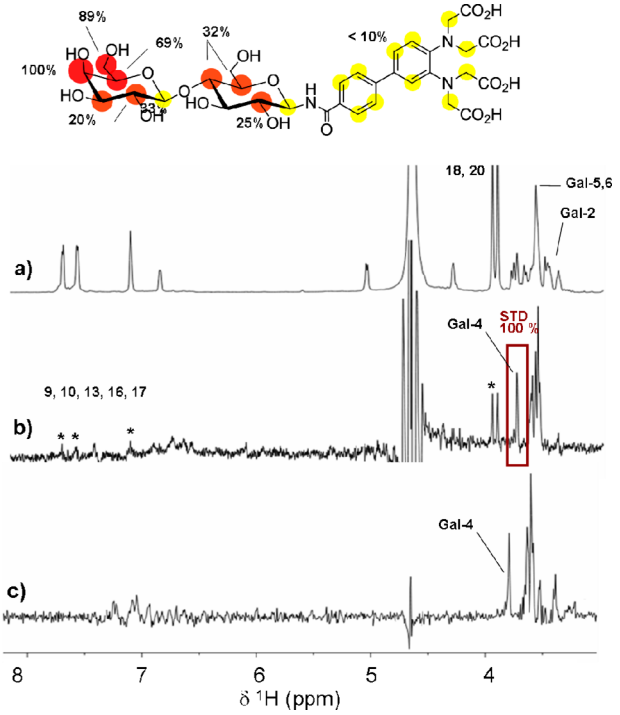

Figure 4. Lower panel: STD experiments performed on either **5** or lactose in the presence of hGal-3 CRD. The sample contains (a) **5**, with labels (off-resonance experiment), (b) hGal3 CRD and **5** (STD experiment), and (c) hGal3 CRD and lactose (STD experiment). Upper panel: ligand epitope mapping of the recognition of **5** by human hGal-3 CRD as inferred from STD experiments. Protons from the PhDTA linker (labeled with asterisks, i.e., aromatic protons 9–17 and those of the chelating arms 18–20) give rise to a much weaker STD response than those from the lactose moiety, thus indicating that the recognition takes place at the level of the sugar.

saturation was received at protons belonging to the galactose unit, especially protons 4–6. A very similar pattern is obtained in STD experiments performed with lactose in the presence of the same protein (Figure 4, C). Taken together, these data indicate that the introduction of the PhDTA linker does not alter the recognition of the sugar by its natural receptor and that the interaction of the conjugate takes place at the level of the sugar moiety.

Regarding the PCS data, the interaction of **5** with hGal-3 CRD was studied from the point of view of the receptor, using the observed chemical shift perturbation data of the protein signals, obtained through $^{1}H-^{15}N$ HSQC experiments.[46] Thus, the ^{15}N-labeled hGal-3 CRD was used for monitoring the binding process. It was expected that the usual chemical shift perturbation data of the $^{1}H-^{15}N$ cross-peaks of hGal-3 in the presence of lactose would be further enhanced in the presence of **5**, due to the presence of the paramagnetic metal ion at the LBT moiety. First, a blank experiment with **5** loaded with La^{3+} was performed, indicating that the chemical shift perturbations induced in the hGal-3 signals were basically identical to those obtained in the presence of just lactose, without the LBT moiety (Figure 3). Thus, the binding modes of **5** and lactose to hGal-3 are equivalent. Then, different protein samples were titrated with increasing amounts of the lactose derivative **5** previously loaded with the chosen paramagnetic ions (Figure 5),

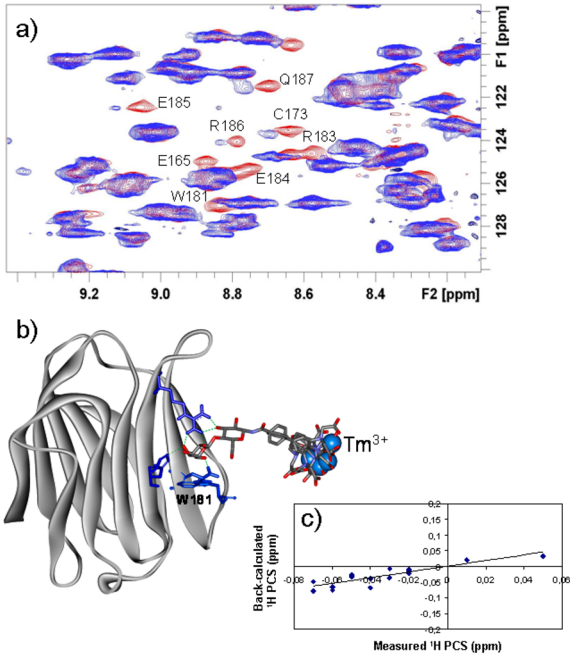

Figure 5. (a) Superimposition of $^{1}H-^{15}N$ HSQC spectra of hGal-3-CRD in complex with 12 equiv of the lactose-analogue **5** acquired in the presence of a diamagnetic metal (red, loaded with La^{3+}) and in the presence of a paramagnetic metal (blue, loaded with Tm^{3+}). Some of the residues with the highest PCSs are labeled. (b) Structure of h-gal3/lactose derivative **5** complex built from the coordinates of PDB 2NN8. Eight structures of the synΦ/synΨ conformer were considered in the calculation to take into account the flexibility of the biphenyl linker. (c) Comparison of the back-calculated PCS (MSpin calculation) for the structure represented in (b) with those experimentally observed.

as described in the Methods section. In detail, for these experiments, two different paramagnetic metals were tested, namely Dy^{3+}or Tm^{3+}.

In both cases, clear PCSs were observed for many protein signals, demonstrating the transfer of the paramagnetic effects to the protein nuclei from the noncovalently bound ligand and thus further assessing the existence of interactions of hGal3 CRD with the carbohydrate analogue. Indeed, both positive and negative chemical shift changes were observed for many $^{1}H-^{15}N$ signals of hGal-3 upon addition of **5** loaded with the different metal ions. In addition, depending on the type of

dx.doi.org/10.1021/ja502406x | J. Am. Chem. Soc. 2014, 136, 8011–8017

metal, some $^{1}H-^{15}N$ cross peaks became broadened and others even disappeared from the spectra, due to PREs. This effect was especially drastic in the case of Dy^{3+}, as expected from its large paramagnetic effects.[19] The overlay of the control spectrum acquired with La^{3+} with the corresponding spectrum acquired with Tm^{3+} is shown in Figure 5.

The results were analyzed on the basis of the available three-dimensional structure of the complex using the X-ray coordinates of the CRD of the hGal-3/lactose complex (PDB code 2NN8).[47] This geometry was used as template to generate the putative complex with compound **5**, by attaching the LBT fragment to the lactose moiety, as described in the Methods section. Interestingly, PCS values higher than 0.02 can be observed for 32 NH signals, even in residues that are 42 Å apart from the metal core (Supporting Information). This data set represents an improvement with respect to the results described with nitroxide spin-labeled carbohydrate analogues.[20] In that case, only perturbation of residues that fall within a radius of 20 Å from the spin label could be detected, and in addition, only intensity losses could be measured for obtaining structural information. As we now report, the use of lanthanide-binding tags attached to the carbohydrate could allow for the measurement of both PREs and PCSs. This fact, in principle, could be used to detect very weak interactions or lead to a more refined structural analysis.

The PCS data obtained for Dy^{3+} and Tm^{3+} exhibited a different pattern of positive and negative values, as expected from their corresponding iso-surface shapes. The obtained PCS values are given in the Supporting Information.

The most affected residues upon addition of **5** loaded with Tm^{3+} are I171, C173, E185, and Q187, (PCSs: −0.06, −0.07, −0.06, and −0.06 ppm, respectively). These protons are located at shorter distances respect to the metal (23.6, 20.2, 19.1, 21.9 Å, respectively). In the case of Dy^{3+}, these signals disappear due to the higher PRE effect of this ion. In this case, the largest PCSs were detected for A146, L147, D148, F157, and S237 (0.04, 0.05, 0.05, 0.05 and 0.05, respectively). These protons are located at 29.7, 27.8, 29.7, 25.9, and 31.3 Å, respectively.

A hallmark of ligand binding in galectins is the C−H/π-interaction of the galactose unit with a properly located Trp residue.[2] This interaction provides specificity and is also useful as sensor for fluorescence-based monitoring of binding.[48] In the case of h-Gal3, W181 and the galactose moiety of lactose are in close contact. Due to its proximity to the metal ion (NH-metal distance 16 Å), the backbone NH of this residue is one of the most affected upon ligand binding and disappears in all the spectra acquired with the carbohydrate conjugate loaded with the paramagnetic metal ions (Tm^{3+}or Dy^{3+}). It is worth noting that this is one of the few signals that becomes broadened below detection in the experiment with Tm^{3+}. In fact, the data measured with the carbohydrate conjugate loaded with Tm^{3+} (metal with the lowest PRE of the two employed) were very useful to characterize the protein−carbohydrate interaction surface. Therefore, the combination of data obtained with the different metals led to an improved definition of the binding event.

Finally, in order to rule out the possibility of a different binding mode for **5** to that of lactose, competition experiments with lactose were carried out. Lactose was added to hGal-3 samples containing **5**. In the presence of lactose, the amide NH signals in the $^{1}H-^{15}N$ HSQC spectrum of hGal-3 shifted back toward the chemical shift values of the blank sample (lactose loaded with La^{3+}). Furthermore, those cross peaks that had disappeared or had shown a large line broadening in the presence of **5** loaded with either Tm^{3+} or Dy^{3+} could be observed again (see Supporting Information). This result shows that **5** and lactose compete for the same binding site, further assessing the existence of equivalent binding modes, and, therefore, that the interaction of 5 with hGal-3 is specific.

Finally, MSpin calculations were carried out to further confirm that the experimental PCSs for the hGal3 CRD in the presence of **5** are in agreement with those expected for the known X-ray structure of the hGal3/lactose complex. The hGal3/lactose complex PDB 2NN8 was used as starting point to build the structure of hGal3/**5** complex. In these coordinates, lactose is in the synΦ/synΨ conformation. Different rotamers of the biphenilic moiety and the bond connecting the amide adjacent to the aromatic ring were considered to take into account the linker flexibility in the calculations, as described above for the lactose derivative in the free state. In all cases, the back-calculated PCSs for the protein signals were in very good agreement with the experimental data. MSpin Q factors were 0.3 and 0.2 for Tm^{3+} and Dy^{3+}, respectively (Figure 5C and Supporting Information).

CONCLUSION

A novel lanthanide-binding tag has been designed to functionalize carbohydrate moieties maintaining their possible bioactivity via lectin binding. Loading the chelating part with two paramagnetic ions enabled to efficiently determine the conformation of a model disaccharide (lactose) by using PCS data, independent of NOEs and J-couplings. Beyond conformational characterization of the ligand, bound-state topological features of a carbohydrate binding protein can also be defined. Paramagnetic effects of the metal ion are sensed by the protein as evidenced in the PCS values of the cross peak signals in $^{1}H-^{15}N$ HSQC spectra. In this case, both PRE and PCS effects can be transferred from the LBT-decorated carbohydrate to the protein, provided that the protein accommodates the carbohydrate. Since the chemical shift perturbations induced by the carbohydrate at the binding site of the protein and its periphery are enhanced by the PCS effects of the metal present at the LBT, detection of molecular interactions can readily be performed. This approach may be particularly useful for detecting low-affinity events or transient interactions. Furthermore, a detailed analysis of the data may permit the proper location of the binding site, provided that a putative geometrical model is available.

Using this methodology, screening for lectin-blocking compounds can thus be advanced, since detection of secondary sites can be accomplished. Of particular relevance, comparative analysis within a lectin family, in our case adhesion/growth-regulatory galectins, is readily possible with such a sensor, probing into lectin differences. Moreover, feasibility of studies on other carbohydrate-binding proteins such as glycoenzymes or transporters markedly broadens the scope of possible applications.

Finally, this approach constitutes an attractive alternative to the use of protein tagging. In our case, no protein engineering is required, thus allowing for the study of the protein in its native form.

ASSOCIATED CONTENT

Supporting Information

Protein purification protocol. Synthesis and chemical characterization of **5** and intermediates. Dissociation constant calculations obtained from the NMR titrations. Description of the MSpin calculations. Detailed table with the PCSs measured with the different metal ions (Tm^{3+} and Dy^{3+}) and parameters of the calculated $\Delta\chi$ tensors. This material is available free of charge via the Internet at http://pubs.acs.org.

dx.doi.org/10.1021/ja502406x | J. Am. Chem. Soc. 2014, 136, 8011−8017

AUTHOR INFORMATION

Corresponding Author

jjbarbero@cib.csic.es

Notes

The authors declare no competing financial interest.

ACKNOWLEDGMENTS

This research was financially supported by funding from the EC Seventh framework program FP7/2007-2013 under REA grant agreements no. 260600 (GlycoHIT) and 317297 (GLYCOPHARM), MHit project of the Comunidad de Madrid, Spain, CTQ2012-32025, CTQ2012-31063 projects, and Ramon y Cajal grant to Dr. Angeles Canales from the Spanish government. We would also like to thank the NMR facility of the Universidad Complutense de Madrid (CAI) and the company MestreLab Research for making MSpin software available. M.A.B. acknowledges an FPI fellowship from the Spanish Ministry of Economy and Competitiveness.

REFERENCES

(1) Gabius, H. J. *The Sugar Code: Fundamentals of Glycosciences* Wiley-VCH: Weinheim, 2009.

(2) Gabius, H. J.; André, S.; Jiménez-Barbero, J.; Romero, A.; Solis, D. *Trends Biochem. Sci.* **2011**, *36*, 298−313.

(3) Chabre, Y. M.; Giguere, D.; Blanchard, B.; Rodrigue, J.; Rocheleau, S.; Neault, M.; Rauthu, S.; Papadopoulos, A.; Arnold, A. A.; Imberty, A.; Roy, R. *Chemistry* **2011**, *17*, 6545−62.

(4) Prost, L. R.; Grim, J. C.; Tonelli, M.; Kiessling, L. L. *ACS Chem. Biol.* **2012**, *7*, 1603−8.

(5) Arda, A.; Blasco, P.; Varon Silva, D.; Schubert, V.; André, S.; Bruix, M.; Canada, F. J.; Gabius, H. J.; Unverzagt, C.; Jimenez-Barbero, J. *J. Am. Chem. Soc.* **2013**, *135*, 2667−75.

(6) Canales, A.; Lozano, R.; Lopez-Mendez, B.; Angulo, J.; Ojeda, R.; Nieto, P. M.; Martin-Lomas, M.; Gimenez-Gallego, G.; Jimenez-Barbero, J. *FEBS J.* **2006**, *273*, 4716−27.

(7) Garcia-Mayoral, M. F.; Canales, A.; Diaz, D.; Lopez-Prados, J.; Moussaoui, M.; de Paz, J. L.; Angulo, J.; Nieto, P. M.; Jimenez-Barbero, J.; Boix, E.; Bruix, M. *ACS Chem. Biol.* **2013**, *8*, 144−51.

(8) Neuhaus, D.; Williamson, M. P. *The Nuclear Overhauser Effect in Structural and Conformational Analysis*; Wiley-VCH: New York, 2000.

(9) Prestegard, J. H.; Bougault, C. M.; Kishore, A. I. *Chem. Rev.* **2004**, *104*, 3519.

(10) Xia, J.; Margulis, C. J.; Case, D. A. *J. Am. Chem. Soc.* **2011**, *133*, 15252.

(11) Roldos, V.; Canada, F. J.; Jimenez-Barbero, J. *ChemBioChem* **2011**, *12*, 990.

(12) Bernardi, A.; Jimenez-Barbero, J.; Casnati, A.; De Castro, C.; Darbre, T.; Fieschi, F.; Finne, J.; Funken, H.; Jaeger, K. E.; Lahmann, M.; Lindhorst, T. K.; Marradi, M.; Messner, P.; Molinaro, A.; Murphy, P. V.; Nativi, C.; Oscarson, S.; Penades, S.; Peri, F.; Pieters, R. J.; Renaudet, O.; Reymond, J. L.; Richichi, B.; Rojo, J.; Sansone, F.; Schaffer, C.; Turnbull, W. B.; Velasco-Torrijos, T.; Vidal, S.; Vincent, S.; Wennekes, T.; Zuilhof, H.; Imberty, A. *Chem. Soc. Rev.* **2013**, *42*, 4709.

(13) Gabius, H. J.; Siebert, H. C.; André, S.; Jimenez-Barbero, J.; Rüdiger, H. *Chembiochem* **2004**, *5*, 740−64.

(14) Jiménez Barbero, J.; Peters, T. *NMR Spectroscopy of Glycoconjugates*; Wiley-VCH, Weinheim, 2002.

(15) Koenig, S. H.; Brown, R. D., 3rd; Brewer, C. F. *Proc. Natl. Acad. Sci. U S A* **1973**, *70*, 475−9.

(16) Barbieri, R.; Bertini, I.; Cavallaro, G.; Lee, Y. M.; Luchinat, C.; Rosato, A. *J. Am. Chem. Soc.* **2002**, *124*, 5581−7.

(17) Leonov, A.; Voigt, B.; Rodriguez-Castaneda, F.; Sakhaii, P.; Griesinger, C. *Chemistry* **2005**, *11*, 3342−8.

(18) Saio, T.; Ogura, K.; Yokochi, M.; Kobashigawa, Y.; Inagaki, F. *J. Biomol. NMR* **2009**, *44*, 157−66.

(19) Otting, G. *J. Biomol. NMR* **2008**, *42*, 1−9.

(20) Jain, N. U.; Venot, A.; Umemoto, K.; Leffler, H.; Prestegard, J. H. *Protein Sci.* **2001**, *10*, 2393−400.

(21) Zhuang, T.; Leffler, H.; Prestegard, J. H. *Protein Sci.* **2006**, *15*, 1780−90.

(22) Seidel, R. D., 3rd; Zhuang, T.; Prestegard, J. H. *J. Am. Chem. Soc.* **2007**, *129*, 4834−9.

(23) Zhuang, T.; Lee, H. S.; Imperiali, B.; Prestegard, J. H. *Protein Sci.* **2008**, *17*, 1220−31.

(24) Amano, M.; Eriksson, H.; Manning, J. C.; Detjen, K. M.; André, S.; Nishimura, S.; Lehtio, J.; Gabius, H. J. *FEBS J.* **2012**, *279*, 4062−80.

(25) Diez-Revuelta, N.; Velasco, S.; André, S.; Kaltner, H.; Kübler, D.; Gabius, H. J.; Abad-Rodriguez, J. *J. Cell. Sci.* **2010**, *123*, 671−81.

(26) Kaltner, H.; Gabius, H. J. *Histol. Histopathol.* **2012**, *27*, 397−416.

(27) Krzeminski, M.; Singh, T.; André, S.; Lensch, M.; Wu, A. M.; Bonvin, A. M.; Gabius, H. J. *Biochim. Biophys. Acta* **2011**, *1810*, 150−61.

(28) Quattroni, P.; Li, Y.; Lucchesi, D.; Lucas, S.; Hood, D. W.; Herrmann, M.; Gabius, H. J.; Tang, C. M.; Exley, R. M. *Cell Microbiol.* **2012**, *14*, 1657−75.

(29) Sanchez-Ruderisch, H.; Fischer, C.; Detjen, K. M.; Welzel, M.; Wimmel, A.; Manning, J. C.; André, S.; Gabius, H. J. *FEBS J.* **2010**, *277*, 3552−63.

(30) Saio, T.; Ogura, K.; Shimizu, K.; Yokochi, M.; Burke, T. R., Jr.; Inagaki, F. *J. Biomol. NMR* **2011**, *51*, 395−408.

(31) Mallagaray, A.; Canales, A.; Dominguez, G.; Jimenez-Barbero, J.; Perez-Castells, J. *Chem. Commun. (Camb)* **2011**, *47*, 7179−81.

(32) Erdelyi, M.; d'Auvergne, E.; Navarro-Vazquez, A.; Leonov, A.; Griesinger, C. *Chemistry* **2011**, *17*, 9368−76.

(33) (a) Yamamoto, S.; Yamaguchi, T.; Erdelyi, M.; Griesinger, C.; Kato, K. *Chemistry* **2011**, *17*, 9280−2. (b) Canales, A.; Mallagaray, A.; Pérez-Castells, J.; Boos, I.; Unverzagt, C.; André, S.; Gabius, H. J.; Cañada, F. J.; Jiménez-Barbero, J. *Angew. Chem., Int. Ed.* **2013**, *52*, 13789−93.

(34) (a) *MSpin*; Mestrelab Research: Santiago de Compostela, Spain; http://www.mestrelab.com; accessed May 5, 2014. (b) Navarro-Vázquez, A. *Magn. Reson. Chem.* **2012**, *50*, S73−S79.

(35) Asensio, J. L.; Jimenez-Barbero, J. *Biopolymers* **1995**, *35*, 55−73.

(36) Asensio, J. L.; Martin-Pastor, M.; Jimenez-Barbero, J. *Int. J. Biol. Macromol.* **1995**, *17*, 137−48.

(37) Asensio, J. L.; Martin-Pastor, M.; Jimenez-Barbero, J. *J. Mol. Struct.: THEOCHEM* **1997**, *395*−*396*, 245−270.

(38) Martín-Pastor, M.; Espinosa, J. F.; Asensio, J. L.; Jimenez-Barbero, J. *Carbohydr. Res.* **1997**, *298*, 15−49.

(39) Martin-Pastor, M.; Canales, A.; Corzana, F.; Asensio, J. L.; Jimenez-Barbero, J. *J. Am. Chem. Soc.* **2005**, *127*, 3589−95.

(40) Mizuno, M.; Funahashi, S.; Nakasuka, N.; Tanaka, M. *Inorg. Chem.* **1991**, *30*, 1550−1553.

(41) Mayer, M.; Meyer, B. *Angew. Chem., Int. Ed.* **1999**, *38*, 1784−1788.

(42) Zhang, Y.; Yamamoto, S.; Yamaguchi, T.; Kato, K. *Molecules* **2012**, *17*, 6658−71.

(43) Tvaroska, I.; Bleha, T. *Adv. Carbohydr. Chem. Biochem.* **1989**, *47*, 45−123.

(44) Losonczi, J. A.; Andrec, M.; Fischer, M. W. F.; Prestegard, J. H. *J. Magn. Reson.* **1999**, *138*, 334−342.

(45) Meyer, B.; Peters, T. *Angew. Chem., Int. Ed. Engl.* **2003**, *42*, 864−90.

(46) Shuker, S. B.; Hajduk, P. J.; Meadows, R. P.; Fesik, S. W. *Science* **1996**, *274*, 1531−4.

(47) Collins, P. M.; Hidari, K. I.; Blanchard, H. *Acta Crystallogr., Sect. D: Biol. Crystallogr.* **2007**, *63*, 415−9.

(48) Asensio, J. L.; Arda, A.; Canada, F. J.; Jimenez-Barbero, J. *Acc. Chem. Res.* **2013**, *46*, 946−54.